The Electrostatic Expansion of Linear Polyelectrolytes: Effects of Gegenions, Co-ions, and Hydrophobicity

M. Beer and M. Schmidt*

Johannes Gutenberg-Universität Mainz, Institut für Physikalische Chemie, Jakob-Welder-Weg 11, 55099 Mainz, Germany

M. Muthukumar

Polymer Science and Engineering Department, University of Massachusetts, Amherst, Massachusetts 01003

Received July 7, 1997; Revised Manuscript Received September 22, 1997[⊗]

ABSTRACT: The molar mass and ionic strength dependence of the dimensions of hydrophobically modified poly(vinylpyridinium) cations are demonstrated to be almost perfectly described by a theoretical expression derived on the basis of only excluded volume considerations. Generally, the effective charge density of the polyions decreases significantly with increasing hydrophobicity and with increasing polarizability of the gegenions. Unexpectedly, the intrinsic excluded volume effect which becomes dominating at high ionic strength not only depends on the hydrophobicity of the polyion but also significantly increases with decreasing polarizability of the gegenions (i.e., if the iodide gegenions are replaced by chloride gegenions). Measurements in different solvents reveal that the effective charge density does not linearly depend on the dielectric constant in the regime $20 \leq \epsilon \leq 190$. It is shown that the introduction of the electrostatic persistence length leads to less consistent results, although the experimental data could be fitted equally well.

Introduction

The ionic strength dependence of the dimensions of polyelectrolytes is still a subject of controversial theoretical arguments and experimental results.[1] Early viscosity investigations seemed not to be compatible with the electrostatic excluded volume theories at the time[2−4] and subsequently the concept of the electrostatic persistence length (OSF-model) as developed by Odjik,[5] Skolnick and Fixman,[6] and Le Bret[7] has advanced to a widely accepted basis for the interpretation of various experimental results during the last 20 years. However, precise light-scattering results on various polyelectrolyte systems were not compatible to the predictions of the OSF-model, which has initiated modifications of the OSF-model in terms of the intrinsic and electrostatic excluded volume.[8,9] Eventually, decent fits of the radius of gyration as a function of the ionic strength could be achieved for a variety of different polyions.[9−14] Very recently, the applicability of the OSF-concept (i.e., the electrostatic stiffening) to intrinsically flexible polyions has been questioned by theoretical arguments[15] as well as by simulation results.[16]

The experimental concept of the present work is to collect a systematic and comprehensive set of data in order to experimentally quantify effects of chain length, ionic strength, hydrophobicity, gegenions, and co-ions onto the dimensions of polyelectrolytes in dilute aqueous and organic solutions. As in previous investigations[17−19] we utilize well-defined, anionically prepared poly(2-vinylpyridine)s (PVP) in a wide molar mass regime. The hydrophobicity of the investigated polycations is varied by the quaternization reaction of the respective PVP with acid, with benzyl bromide, and with ethyl, butyl, and octyl iodide.

Theory

Theories of conformations of polyelectrolytes fall into two groups. In the first group[5−8,20−23] the chain is assumed to be a stiff chain and calculations are performed to obtain the effect of the electrostatic interaction between charges on the chain backbone. In the second category,[4,24−26] the chain is assumed to be a flexible chain and the consequence of electrostatic interaction is calculated. We compare our experimental data with the prediction of these two types of theories in the next section. To date, there is no satisfactory theory in the literature to describe the electrostatic effect on conformations of polyelectrolyte chains with arbitrary intrinsic stiffness.

The effect of electrostatic interaction on a flexible polyelectrolyte chain in infinitely dilute solution has been modeled by the following parameters. The chain contains N Kuhn segments with step length l. The total charge on the chain, $lNfeZ/a$, is assumed to be uniformly distributed along the chain backbone, where f is the degree of ionization, a is the monomer length, Z is the valence of the ionic group, and e is the electronic charge. The interaction energy $V(r)$ between the segments separated by a distance r is taken as

$$\frac{V(r)}{k_B T} = w\delta(r) + Z^2 f^2 l_B e^{-\kappa r}/r \qquad (1)$$

where the first and second terms on the right-hand side describe the usual short-ranged excluded volume effect and the electrostatic interaction, respectively. w is the pseudopotential and is equivalent to $(^1/_2 - \chi)l^3$ with χ being the Flory−Huggins interaction parameter. $\delta(r)$ is the Dirac delta function. l_B is the Bjerrum length $e^2/4\pi\epsilon_r\epsilon_0 k_B T$, where ϵ_r is the relative effective dielectric constant of the solution, ϵ_0 is the permittivity of the vacuum, and $k_B T$ is the Boltzmann constant times the absolute temperature. κ is the inverse Debye length given by

$$\kappa^2 = 4\pi l_B (Z_c^2 c_c + \sum_\gamma Z_\gamma^2 c_\gamma) \qquad (2)$$

where Z_c and c_c are respectively the valence and the

[⊗] Abstract published in *Advance ACS Abstracts,* November 15, 1997.

S0024-9297(97)00982-0 CCC: $14.00

number concentration of the counterion to the polyelectrolyte. Z_γ and c_γ are the valence and number concentration of γth salt ion.

Assuming a uniform expansion for the chain and utilizing a variational procedure,[25,26] the expansion factor α for the radius of gyration was derived to be

$$\alpha^5 - \alpha^3 = w_0 N^{1/2} + \frac{134}{105}\sqrt{6}\frac{Z^2 f^2 l_B}{l} N^{3/2}\alpha^2 \left\{ \frac{e^a}{2a^{5/2}}(a^2 - 4a + 6)\mathrm{erfc}\sqrt{a} + \left(-\frac{3}{a^{5/2}} - \frac{1}{a^{3/2}} + \frac{6}{\sqrt{\pi a^2}} \right) \right\} \quad (3)$$

where

$$a = \kappa^2 l^2 N \alpha^2/6 \quad \text{and} \quad w_0 = \frac{134}{105}\left(\frac{3}{2\pi}\right)^{3/2}\left(\frac{1}{2} - \chi\right)$$

If $\kappa^2 l^2 N\alpha^2/6 \gg 1$ eq 3 reduces to

$$\alpha^5 - \alpha^3 = \left[w_0 + \frac{134}{35}\sqrt{\frac{6}{\pi}}\frac{l_B}{l}\frac{Z^2 f^2}{\kappa^2 l^2} \right]\sqrt{N} \quad (4)$$

Equation 4 is equivalently written in the form of the modified Flory formula,[29] as

$$\alpha^5 - \alpha^3 = \frac{134}{105}\left(\frac{3}{2\pi}\right)^{3/2}\left[\left(\frac{1}{2} - \chi\right) + 4\pi\frac{l_B Z^2 f^2}{\kappa^2 l^3} \right]\sqrt{N} \quad (5)$$

This result can readily be guessed directly from the equation for $V(r)$. If κ is large, the second term on the right-hand side of eq 1 becomes short-ranged, $4\pi Z^2 f^2 l_B \kappa^{-2}\delta(r)$ so that the effect of added salt is only to change the value of w_0 as shown in the bracket term of eq 4. This point has already been noted by Flory.[24]

On the other hand, if $\kappa^2 l^2 N\alpha^2/6 \ll 1$, eq 3 reduces to

$$\alpha^3 - \alpha = \frac{w_0}{\alpha^2}N^{1/2} + \frac{134}{(105)(15)}\sqrt{\frac{6}{\pi}}\frac{Z^2 f^2 l_B}{l}N^{3/2} \quad (6)$$

For Θ solutions ($w_0 = 0$) and for $N \gg 1$, but still maintaining the condition of $\kappa^2 l^2 N\alpha^2/6 \ll 1$, eq 6 reduces to

$$\alpha = \left(\frac{134}{1575}\right)^{1/3}\left(\frac{6}{\pi}\right)^{1/6}\left(\frac{Z^2 f^2 l_B}{l}\right)^{1/3} N^{1/2} \quad (7)$$

so that the radius of gyration R_g follows as

$$R_g = \left(\frac{134}{1575}\right)^{1/3}\left(\frac{6}{\pi}\right)^{1/6}\frac{1}{\sqrt{6}}(Z^2 f^2 l^2 l_B)^{1/3} N \quad (8)$$

with the same scaling form as originally obtained by Kuhn, Künzle, and Katchalsky[27] which in turn has recently been interpreted using the electrostatic blob model.[28]

Equation 3 provides a smooth crossover between the good solution behavior for $\kappa R_g \gg 1$ and the rod-like behavior for $\kappa R_g \ll 1$. In order to compare the theoretical prediction with experimental data, it is to be remembered that there are three dimensionless variables, $w_0 N^{1/2}$, $Z^2 f^2 l_B N^{3/2}/l$, and $\kappa l\sqrt{N}$. Care must be exercised in comparing data with theory in the various crossover regions. For most of the experimental data reported in this paper, $\kappa R_g > 1$ so that we proceed to compare the data with eq 4. w_0 and f are taken to be unknown parameters to fit the experimental data.

The alternative method[9] of analyzing the data is based on the treatment by Odijk and Houwaart[8] of the excluded volume effect on the electrostatic stiffening of semiflexible chains. The total persistence length l of a stiff polyelectrolyte is the sum of the intrinsic persistence length $l_p \equiv l/2$ and the electrostatic persistence length l_e,

$$l_t = l_p + l_e \quad (9)$$

As shown by Odijk[5] and Skolnick and Fixman,[6]

$$l_e = \frac{1}{4 l_B \kappa^2} \quad (10)$$

in the limit of $\kappa l N \gg 1$ and $l_e < l_p$. In addition to the electrostatic persistence length generated by the charge on the chain backbone, Odijk and Houwaart[8] assume further that there is an excluded volume interaction among cylindrical segments each of length $2l_t$ and diameter $4\kappa^{-1}$. In general, the excluded volume parameter z for a flexible chain of N Kuhn segments with Kuhn length l is

$$z = \left(\frac{3}{2\pi l^2}\right)^{3/2}\beta N^{1/2} \quad (11)$$

where β is the excluded volume. Several approximate formulas for the dependence of the expansion factor α on z have been reported in the literature.[29−31] For the specific model of Odijk and Houwaart, β is solely electrostatic in nature and is given as

$$\beta = \beta_{el} = 8\pi\kappa^{-1} l_t^2 \quad (12)$$

Combining with the Yamakawa−Tanaka equation[29] for α in terms of z,

$$\alpha^2 = 0.541 + 0.459\,(1 + 6.04z)^{0.46} \quad (13)$$

Equations 11 and 12 lead to the result

$$R_g^2 = \frac{L}{3}[l_p + (4 l_B \kappa^2)^{-1}](0.541 + 0.459\{1 + 4.43 L^{1/2}\kappa^{-1}[(4 l_B \kappa^2)^{-1}]^{-3/2}\}^{0.46}) \quad (14)$$

Here L is the contour length of the chain. In an effort to generalize eq 14 for non-Θ-solutions, Reed et al.[9] have provided an ad hoc treatment by combining theories of Odijk, Odijk and Houwaart, Skolnick and Fixman, and Gupta and Forsman.[32] Here they append an additional contribution β_0 to β, arising from short-ranged nonelectrostatic interactions, so that β of eq 11 is given by

$$\beta = \beta_{el} + \beta_0 \quad (15)$$

where β_0 is taken to be an adjustable parameter (β_0 being actually $^1/_2 - \chi$). In addition, Reed et al. use the empirical formula of Gupta and Forsman[32] (based on Monte Carlo results)

$$\alpha^5 - \alpha^3 = \frac{134}{105}(1 - 0.885 N^{-0.462})z \quad (16)$$

instead of the Yamakawa−Tanaka formula, in evaluating the expansion factor. It must be noted that the applicability of eqs 9−16 is constrained by the basic assumption that the electrostatic persistence length l_e

Table 1. Characterization of the Poly(2-vinylpyridine)s

sample	M_w (THF/MeOH)/g mol^{-1}	L_w/Å	M_w/M_n[a]	R_g/nm	R_h/nm
PVP4000	1.68×10^5	4000	1.13	15.6	9.9
PVP6900	$(2.9 \times 10^5)/(2.8 \times 10^5)$	6900	1.24	17	14.5
PVP10000	4.2×10^5	10 000	1.11	25.4	16.6
PVP18000	$(7.6 \times 10^5)/(7.5 \times 10^5)$	18 000	1.20	37.5	26
PVP21000	8.8×10^5	21 000	1.14	39	27

[a] Determined by GPC in DMF, polystyrene calibration.

Table 2. Degree of Ionization *Q* Determined by Elemental Analysis and by IR Spectroscopy

	C%	H%	N%	Cl,Br%	Q_{EA}[a]	Q_{IR}[b]
Bz-PVP21000Br						77
Bz-PVP18000Br	58.3	5.25	5.72	31.0	95	86
Bz-PVP10000Br	57.2	5.50	5.48	31.7	101	91
Bz-PVP6900Br	58.0	5.96	5.71	30.3	93	86
Bz-PVP4000Br	58.8	5.42	5.56	30.0	94	96
Et-PVP18000Cl	67.7	7.53	9.63	15.6	64	67
Et-PVP10000Cl	67.9	7.34	10.4	14.4	55	58
Et-PVP4000Br	56.6	5.98	8.36	29.4	61	58
Bu-PVP18000Br	53.7	6.08	7.1	32.6	80	67
Oc-PVP18000Br	58.2	7.02	6.33	28.5	79	91

[a] Degree of ionization determined by elemental analysis via the N to Br or Cl ratio. [b] Determined by IR-spectroscopy according to Figure 1a + 1b.

is smaller than the intrinsic persistence length l_p. Therefore care must be exercised in comparing the experimental data with the predictions of eqs 9−16 to make sure that the salt concentration is high enough so that $l_e < l_p$.

Experimental Section

Samples and Sample Preparation. Poly(styrenesulfonate)s (PSS) and poly(2-vinylpyridine)s (PVP) were purchased from Polymer Standard Service, Mainz. All PVP samples were characterized by static and dynamic light scattering in THF, the results of which are shown in Table 1. The exact molar mass determination of the PVP is essential for the goal of the present investigation because the contour length of the polyelectrolyte samples is deducted from the molar mass of the uncharged PVP. In THF the refractive index increment was determined to be $dn/dc = 0.174 \pm 0.001$ mL/g which corrects an erroneous number given by one of us in an earlier publication.[19] In order to double-check the molar masses two samples were additionally measured in methanol where dn/dc was determined to be $dn/dc = 0.261 \pm 0.004$ mL/g. Such precise dn/dc measurements have become possible utilizing an interferometric device designed by Becker et al.[33] Gel permeation chromatography (GPC) measurements in dimethylformamide (DMF) confirmed the narrow molar mass distribution expected for anionically prepared polymers and are included in Table 1.

The quaternization reaction was performed in DMF with ethyl, butyl, and octyl iodide, and in nitromethane with benzyl bromide as follows:

Typically 5 g of PVP was dissolved in 500 mL of DMF. After the addition of 60−100 g of ethyl, butyl, or octyl iodide, respectively, the solution is stirred for several days (typically 4) at 60 °C. The product is precipitated with ether and several times reprecipitated from methanol/ether solutions. In the case of octyl iodide the product precipitates after 3 days of reaction. Then the precipitate is washed with ether, dried, dissolved in DMF, and stirred for about 30 s over an Amberlyt MB3 mixed bed ion exchange resin in order to remove excess iodide ions. After the removal of the ion exchange resin, the reaction is continued by the addition of 50 g of octyl iodide for 3 more days.

The reaction with benzyl bromide is performed in nitromethane for 8 weeks at ambient temperature as described earlier.[11] Control experiments revealed that no degradation of the PVP occurs under the applied reaction conditions, i.e., the molar mass of the PVP did not change when heated to 70 °C in DMF for 2 weeks.

For all samples the exchange of gegenions is performed by ultrafiltration with Amicon Diaflo YM3 membranes.

Throughout the paper we utilize the following abbreviations for the samples: Al-PVPL_wX with Al the alkylation agent (H for hydrogen, Et for ethyl, Bu for butyl, Oc for octyl, and Bz for benzyl), L_w the contour length in Å, and X the gegenion.

The degree of quaternization was determined by elemental analysis and by IR spectroscopy. Table 2 shows the results of elemental analysis to be always short on C, but to exhibit an excess of N and Br or Cl, respectively. The degree of quaternization has been derived from the ratio Br/N or Cl/N and might be subject to a considerable uncertainty. Therefore, the degree of quaternization was also determined by IR spectroscopy by the ratio of the absorption peaks at 1620 and 1590 cm^{-1} as demonstrated by Figure 1a,b. Calibration was achieved by defined mixtures of an unquaternized PVP sample with the Bz-PVP10000Br of "known" degree of quaternization. In order to experimentally determine the absolute degree of quaternization of sample Bz-PVP10000Br by an alternative method we tried to precisely measure the absolute molar mass of the sample by light scattering in the dialysis equilibrium in a 0.01 M NaBr solution. For this measurement the water content of the sample was determined to be 5% by Karl Fischer and the refractive index increment was determined to be $dn/dc = 0.191$ mL/g. From the increase in molar mass ($M_w = 1.06 \times 10^6$ g/mol) as compared to the "parent" PVP ($M_w = 4.2 \times 10^5$ g/mol) the degree of quaternization was calculated to be 91%. The result of both methods, elemental analysis and IR spectroscopy, agree within the relatively large uncertainty of 10%, but lie well above the Manning condensation limit of 35%. The protonated PVPs were prepared by simple dissolution in the respective acids at pH = 3. According to literature[34] this leads to degrees of protonation of close to 30%.

For the PSS samples the dn/dc value was determined to be $dn/dc = 0.195$ at $c_s = 0.03$ M (NaCl) under dialysis equilibrium. The light-scattering characterization of the PSS samples is given in Table 3.

Static and Dynamic Light Scattering. Static and dynamic light-scattering measurements were performed with an ALV-Sp86 goniometer and an ALV3000 correlator. A Kr-ion laser (Spectra-Physics, 2025−11) operating at 647.1 nm wavelength was used as the light source (output power 500 mW). The performance of the instrument and data evaluation is described in detail elsewhere.[19] Particularly for measurements at high salt concentrations the refractive index of the solution and of the solvent viscosity were corrected with respect to the pure solvent values.

Concentration Regime of the Light-Scattering Measurements. As stated very clearly in earlier publications,[1,19] measurements should be performed in a certain regime of

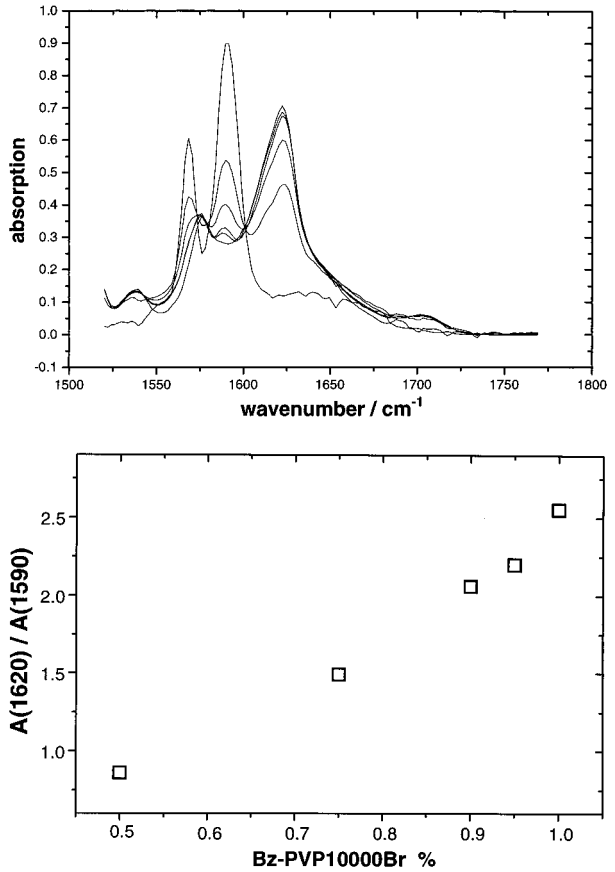

Figure 1. (a) IR-spectrum of mixtures of poly(2-vinylpyridine) and the quaternized sample Bz-PVP10000Br. From bottom to top (at 1620 cm^{-1}): 100% PVP, 50% PVP, 25% PVP, 10% PVP, 5% PVP, and 0% PVP. (b) Ratio of the IR-peak intensities from 1620 to 1590 cm^{-1} as a function of the weight fraction of the sample Bz-PVP10000Br. For absolute calibration the degree of ionization of Bz-PVP10000Br is determined to 91% (see Experimental Section).

Table 3. Characterization of the Sodium Poly(styrenesulfonate) Samples in 0.01 M Aqueous NaCl Solution

sample	M_w/(g mol^{-1})	R_g/nm	R_h/nm	M_w/M_n[a]
PSS400	4.0×10^5	45.5	24.9	1.1
PSS780	5.7×10^5	61.2	30.8	1.1

[a] As given by the supplier.

polyion and salt concentration in order to monitor single polyion properties:

(1) The polyion concentration should lie below the overlap concentration $c_p^* = 3M_w/(4\pi N_A R_g^3)$. For the present measurements the largest of a series of 3−5 concentrations is well below c^*, i.e., $c_p < 0.15c^*$.

(2) Electrostatic interparticle interactions should not contribute to the scattering intensity via the interparticle structure factor. This is safely excluded by restricting the measurements to above 10^{-3} M added salt. Defining the mean distance between the outer segments of two neighboring polyions as $\Delta d \equiv d_{cm} - 2R_g$ (with d_{cm} the average center of mass distance), we always experimentally verify $\kappa\Delta d > 10$ with κ^{-1} the Debye screening length as defined in eq 2. As shown below, the experimental data do not show a noticeable influence of the interparticle structure factor in terms of a nonlinear dependence of the reduced scattering intensity vs q^2 or in terms of an anomalous concentration dependence.

(3) Above a certain polyion concentration dynamic light-scattering measurements exhibit two diffusive modes. The fast one is safely attributed to single-ion diffusion which at higher c_p couples to the counterion dynamics. The origin of the slow mode is not understood at all, but it inevitably falsifies the scattering intensity.[1,18] The occurrence of the slow mode

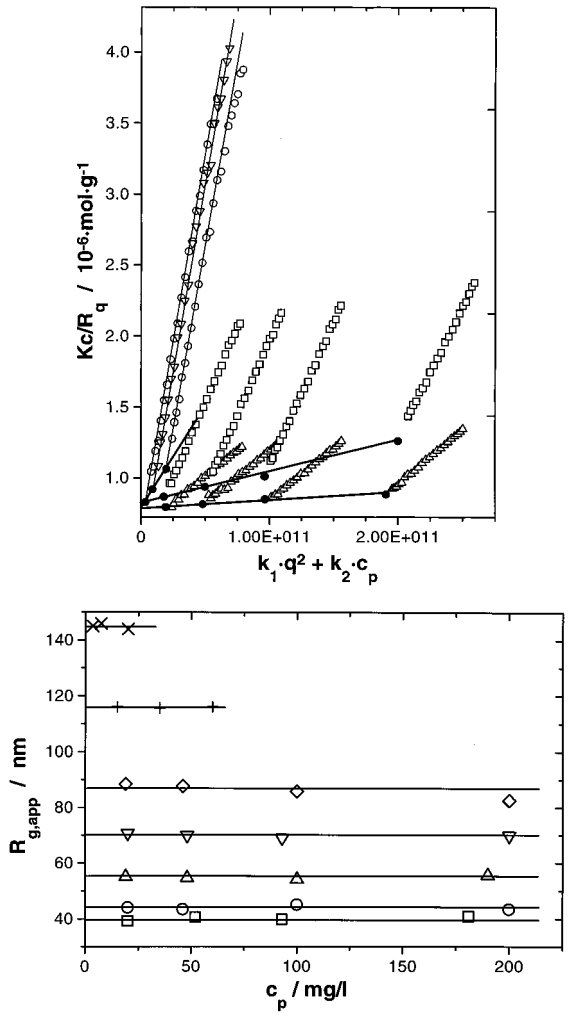

Figure 2. (a) Zimm plots of sample Et-PVP18000Br at different concentrations of added salt: (△) $c_s = 0.1$ M, 20 mg/L ≤ c_p ≤ 200 mg/L; (□) $c_s = 0.01$ M, 20 mg/L ≤ c_p ≤ 200 mg/L; (○) (▽) $c_s = 10^{-3}$ M, c_p = 4, 8, and 19 mg/L. The abcissa is dimensionless with $k_1 = 1$ cm^2 and $k_2 = 10^9$ L/g. (b) Apparent radius of gyration $R_{g,app}$ defined by eq 17b as a function of the polyion concentration c_p for different added salt concentrations c_s: 10^{-3} M (×); 3×10^{-3} M (+); 10^{-2} M (◊); 3×10^{-2} (▽); 0.1 M (△); 0.3 M (○); 1 M (□).

in all presently investigated samples irrespective of hydrophobicity and type of gegenions is shown to occur at $c_p^m/c_s \approx 1$with c_p^m the molar concentration of monomers of the polyions in solution (see Figures 11a−c) and related discussion below). Accordingly, all measurements were performed in a concentration regime $c_p^m < 0.1c_s$which at low salt concentrations is more restrictive than the condition $c_p < c_p^*$.

In order to demonstrate the extremely painful experimental procedures a Zimm-plot of the measurements on sample Et-PVP18000Br is shown in Figure 2a at $c_s = 0.1$, 0.01, and 0.001 M added NaBr. The corresponding radii of gyration are plotted in Figure 2b as a function of polyion concentration. It is recognized that the uncertainty of the measurements hardly exceeds the size of the symbols despite the extremely low concentrations measured. We here also wish to correct a misinterpretation of one of us in an earlier work[19] where a steep upturn of R_g with decreasing c_p was reported. At the time this was interpreted as the onset of interparticle interaction. It has now been recognized that the upturn artificially originates from the evaluation of R_g as

$$R_g^2(c) = 3\left[\frac{d(Kc/R_\Theta)}{dq^2}\Big/\frac{Kc}{R_{\Theta=0}}\right]_{c=c_p} \qquad (17a)$$

whereas in Figure 2b R_g is defined as

$$R_g^2(c) \equiv 3\,\frac{d}{dq^2}\left[\frac{Kc}{R_\Theta}\right]_{c=c_p}\Bigg/\left[\frac{Kc}{R_{\Theta=0}}\right]_{c_p=0} \qquad (17b)$$

The latter definition eliminates the strong concentration dependence caused by the extremely large virial coefficient.

Results and Discussion

Effect of Hydrophobicity. The ionic strength dependence of the polyelectrolyte dimensions for different molar masses are shown in Figures 3−5 for the H-PVP, Et-PVP, and Bz-PVP samples, respectively. In all these measurements the gegenion is Br^- and the added salt is NaBr. It is qualitatively recognized that almost all data sets exhibit a constant slope at small c_s irrespective of the hydrophobicity of the polyelectrolyte. The exponents observed vary between −0.15 and −0.24 with the tendency that the slope increases with decreasing hydrophobicity and increasing chain length. The slopes are somewhat smaller than those reported for NaPSS.[9,10] On the contrary at high salt concentration the hydrophobicity becomes the dominating parameter which determines the curvature of the plots and the solubility limit ("salting out effect"). In terms of the theoretical expression given by eq 4 the charge density f dominates at low c_s whereas w_0 essentially controls curvature and precipitation point at high c_s. The theoretical curves shown in Figures 3−5 are observed to almost perfectly fit the experimental points for polyelectrolyte chain length smaller than $L_w \leq 10^4$ Å, whereas for the two longer chains ($L_w = 1.8 \times 10^4$ and $L_w = 2.1 \times 10^4$ Å) a significant mismatch between experimental data and theoretical curves is observed, irrespective of the hydrophobicity of the polyelectrolyte particularly at low salt concentration. These deviations are also corroborated by the dynamic light-scattering data discussed in Appendix B. By extracting the hydrodynamic radius R_h from the measured diffusion coefficient the ratio of R_g/R_h is found to be in the range of 2−2.4 at low salt concentrations $c_s < 10^{-2}$ M. This range for R_g/R_h is consistent with chain conformations being more expanded than expected for chains with self-avoiding walk statistics.

These systematic deviations are not too surprising since eq 4 is an asymptotic result, only. As noted in the theoretical section, the various dimensionless parameters are $w_0\sqrt{N}$, $Z^2f^2l_BN^{3/2}/l$ and $\kappa l\sqrt{N}$. When $\kappa l\sqrt{N} \gg 1$, there are only two variables. The first is $w_0\sqrt{N}$ and the second is the ratio of $Z^2f^2l_BN^{3/2}/l$ to the square of $(\kappa l\sqrt{N})^2$, which is $(Z^2f^2l_B\sqrt{N}/\kappa^3l^3)$ as exhibited in eq 4. However, if $\kappa l\sqrt{N}$ is not much larger than unity, the asymptotic form of eq 4 is not valid and systematic deviations occur. The chain expands more than predicted by eq 4 as $Z^2f^2l_BN^{3/2}/l$ increases at lower values of $\kappa l\sqrt{N}$.

The values for f and w_0 derived from the theoretical curves (solid lines in Figures 3−5) are summarized in Table 4 and display the following qualitative features:

The value of w_0 for the most hydrophilic H-PVP samples is zero or slightly below zero, indicating that the H-PVP chains should adopt an "unperturbed" conformation at high salt concentrations.

The slightly more hydrophobic Et-PVP exhibits a slightly smaller w_0-value, whereas Bz-PVP with $w_0 = -0.32$ represents the most hydrophobic polyelectrolyte. It is to be noted that $w_0 = -0.32$ leads to precipitation at $c_s = 0.13$ M in good agreement with the experimentally observed solubility limit at $c_s = 0.14$ M (see Table 4).

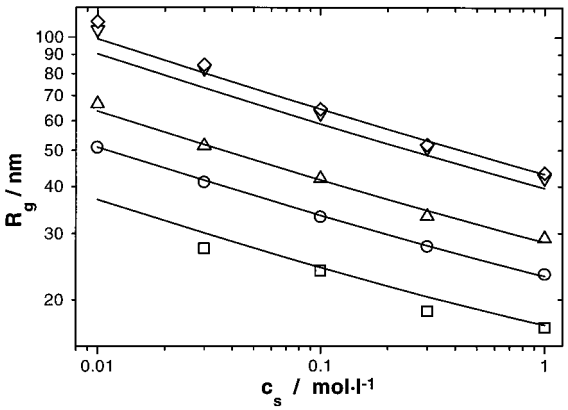

Figure 3. Ionic strength dependence of the radius of gyration for sample H-PVPL_wBr: $L_w = 4000$ Å (□); $L_w = 6900$ Å (○); $L_w = 10\,000$ Å (Δ); $L_w = 18\,000$ Å (▽); $L_w = 21\,000$ Å (◇). The solid lines correspond to the best fit to all data by the theoretical eq 4 with $f = 0.22$ and $w_0 = -0.02$.

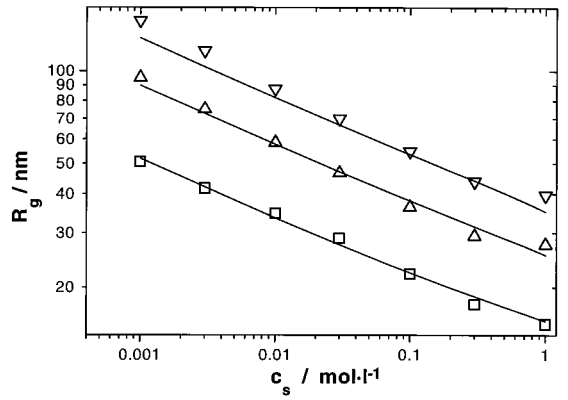

Figure 4. Ionic strength dependence of the radius of gyration for sample Et-PVPL_wBr: $L_w = 4000$ Å (□); $L_w = 10\,000$ Å (Δ); $L_w = 18\,000$ Å (▽). The solid lines are calculated with $f = 0.17$ and $w_0 = -0.03$.

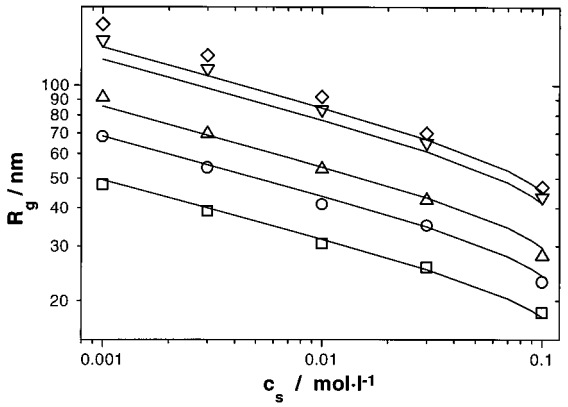

Figure 5. Ionic strength dependence of the radius of gyration for sample Bz-PVPL_wBr: Symbols as in Figure 2. The solid lines are calculated with $f = 0.15$ and $w_0 = -0.32$.

It is most interesting to note that the fitted value for the effective charge density f does significantly depend on the hydrophobicity of the chain and decreases from $f = 0.22$ for H-PVP to $f = 0.15$ for Bz-PVP. Thus, all fitted charge densities lie well below the Manning counterion condensation limit of $f = 0.35$.

The trends discussed above are confirmed by the measurements of butyl- and octyl-quaternized samples which are shown in Figure 6 along with the H-PVP, Et-PVP, and Bz-PVP for the $L_w = 18\,000$ Å polyion. It is qualitatively observed that f as well as w_0 decrease in the sequence H > Et > Bu > Oc. The data on Bz-PVP,

Table 4. Fit parameters w_0 and f for Differently Quaternized Poly(vinylpyridine)s[a]

	f	w_0	c_s^*(theo)	c_s^*(exp)
H-PVPL_wBr	0.22	−0.02	4.5 M	
Et-PVPL_wBr	0.17	−0.03	1.8 M	1−2 M[b]
Bz-PVPL_wBr	0.15	−0.32	0.13 M	0.14 M

[a] The calculated (according to eq 4) and the observed "salting out" concentrations, c_s^*, are also given. [b] Minimum of R_g vs c_s as discussed in the text.

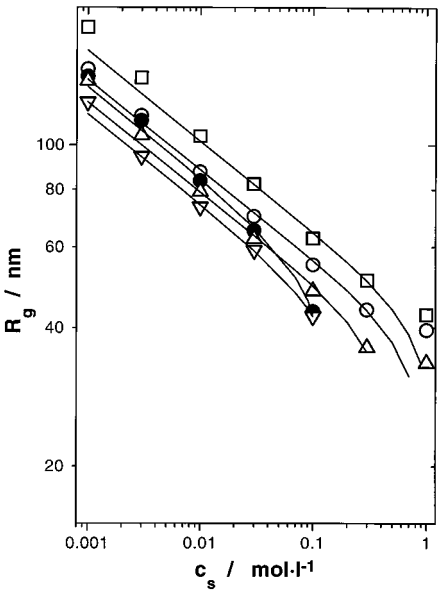

Figure 6. Effect of hydrophobicity on the ionic strength dependence of the radius of gyration for sample Al-PVP18000Br: Al = H (□), Et (○), Bu (Δ), Oc (▽), and Bz (●). The solid lines represent the best theoretical fit, the parameters of which are unreliable as discussed in the text: $f = 0.3$, $w_0 = -0.15$ (H); $f = 0.21$, $w_0 = -0.15$ (Et); $f = 0.17$, $w_0 = -0.17$ (Bu); $f = 0.14$, $w_0 = -0.25$ (Oc); $f = 0.2$, $w_0 = -0.65$ (Bz).

however, seem to show that charge density and hydrophobicity are not necessarily correlated as the charge density is closer to the Et-PVP with w_0 being much more negative.

Unfortunately, only the PVP with $L_w = 18\,000$ Å was quaternized with butyl and octyl groups, thus belonging to the high molar mass polyions which could not be well fitted by the theoretical eq 4 as discussed above. Therefore the fits shown in Figure 6 do not yield f and w_0, quantitatively. Also, significant deviations are observed in the high salt region. These are believed to originate from a strange behavior described in another paper[35,36] that some polyions with I^- gegenions exhibit a "miscibility gap" as a function of added monovalent salt, i.e., after being salted out at a certain c_s^* the polyion dissolves again at a higher salt concentration c_s^{**}. For $c_s > c_s^{**}$ the solubility and the dimension of the polyion increases with increasing c_s. Although such miscibility gaps were already observed long ago[37] on poly(vinylsulfate)s a rigorous explanation for such a phase diagram is still lacking.

For Br-gegenions this miscibility gap is usually not reached because c_s^* is shifted to higher c_s, very close to or higher than c_s^{**}. As a consequence a minimum in the polyion dimension is observed which for the data in Figure 6 is approximately located at $c_s \approx 1-2$ M. Accordingly, we believe the solid line to represent the proper fit for the triangles and the apparent mismatch with the data point at 1 M salt to be caused by the onset of the yet unexplained increase in solvent quality at

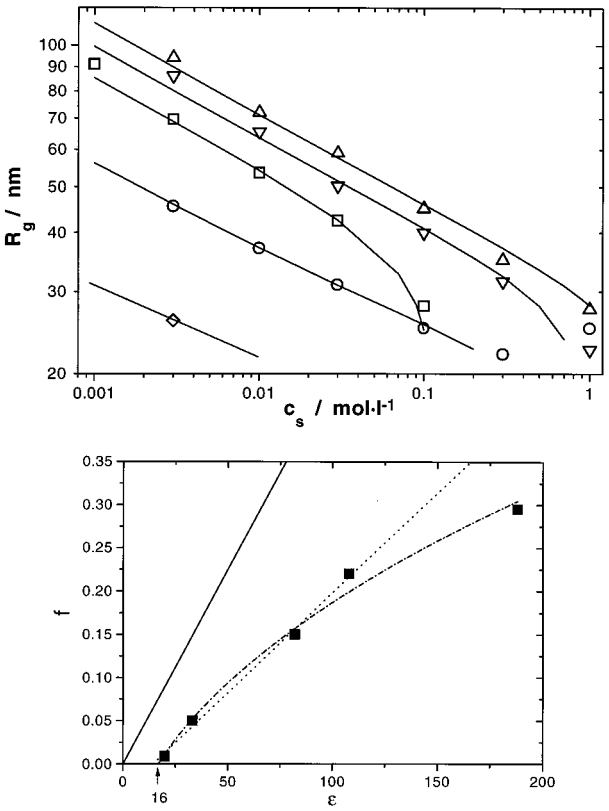

Figure 7. (a) Solvent effect on the ionic strength dependence of the radius of gyration for sample Bz-PVP10000Br: N-methylformamide (Δ), formamide (▽), water (□), methanol (○), and propanol (◊). The fitted values for f and w_0 are listed in Table 5. (b) Effective charge density f as fitted to the experimental data shown in Figure 7a as a function of the dielectric constant of the solvents. The solid line represents the Manning condensation theory, the dotted and dash/dot lines the best fit to a linear and square-root dependence, respectively.

Table 5. Fitted Values for f and w_0 of the Sample Bz-PVP10000Br in Solvents of Different Dielectric Consistent ϵ

	ϵ	f	w_0
1-propanol	20[a]	(<0.01)	(−0.015)
methanol	33[a]	0.05	−0.022
water	82[b]	0.15	−0.3
formamide	108[b]	0.22	−0.22
N-methylformamide	188[b]	0.295	−0.1

[a] Literature values. [b] Determined by dielectric spectroscopy at $f = 100$ kHz at 20 °C. The values in parentheses are estimated from the measurement at $c_s = 0.003$ M and from the observed solubility limit.

higher c_s. For Cl-gegenions such a trend is almost not observable and for F^- this c_s regime is not reached due to the limited solubility of NaF in water (see Figure 8).

Influence of the Solvent Dielectric Constant. In order to derive f and w_0 values in other solvents but water we have investigated the sample Bz-PVP10000Br in propanol, methanol, formamide, and methylformamide (MFA), thus covering a broad range of the dielectric constant $20 \le \epsilon \le 190$. The results are shown in Figure 7a along with the fitted curves according to eq 4. The fit parameters are listed in Table 5. The w_0 values qualitatively describe the solvent quality for the polymer chain bare of any charges or dipoles in the form of nondissociated ion pairs in the sequence which corresponds to the intuitive guess of a chemist. Also the charge density f increases with ϵ as expected. However, the theoretically postulated linear dependence of f vs ϵ is not observed as revealed by Figure 7b.

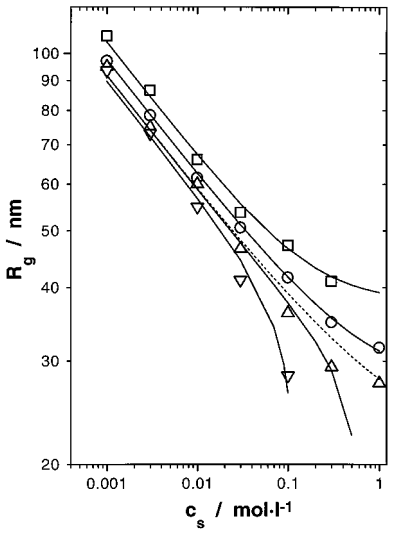

Figure 8. Ionic strength dependence of the radius of gyration for sample Et-PVP10000X with different gegenions: $X^- = F^-$ (□), Cl^- (○), Br^- (Δ), and J^- (▽).

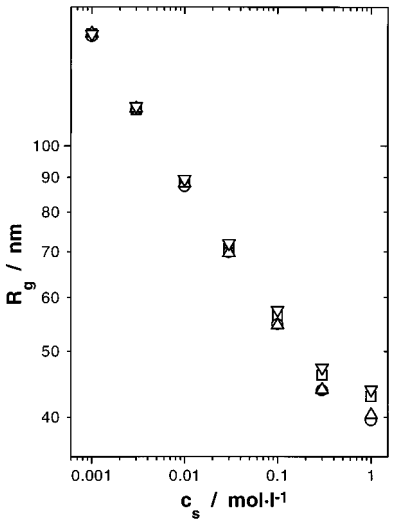

Figure 9. Ionic strength dependence of the radius of gyration for sample Et-PVP18000 Br with different coions: Li^+ (□), Na^+ (○), K^+ (Δ), and Cs^+ (▽).

Rather, a significant downward curvature is observed. All experimental values for f lie significantly below the counterion condensation limit postulated by Manning (full curve in Figure 7b). Also, the experimental curves are seen not to hit the origin, a behavior which is not easily explained. This leads to the question as to whether the fitted charge density represents the true physical or "effective" charge density of the polyelectrolyte chain. As will be shown below the fitted charge density for sodium poly(styrenesulfonate) indeed is close to the expected Manning limit of $f = 0.35$, thus supporting the general reliability of the results.

Effect of Co-ions and Gegenions. The effect of different gegenions and co-ions on the polyion dimensions is shown in Figures 8 and 9, respectively, for the Et-PVP sample with $L_w = 10^4$ Å. Unexpectedly, a huge effect on f and on w_0 is observed when the gegenion is changed from F^- to Cl^- to Br^- to I^-. The curves for the F^-, Cl^-, and I^- gegenions are well fitted by the f and w_0 values listed in Table 6. Only for the Br^- gegenion a significant deviation is observed at high salt concentrations as discussed already above (see Effect of Hydrophobicity) which allows w_0 to vary between $w_0 = -0.012$ (full curve for Δ in Figure 8) and $w_0 = 0$ (dotted curve).

Table 6. Fitted Values for f and w_0 for the Sample Bz-PVP10000X with Different Gegenions X^-

X^-	f	w_0
F^-	0.25	+0.5
Cl^-	0.21	0.0
Br^-	0.18	−0.012/0.0
J^-	0.17	−0.5

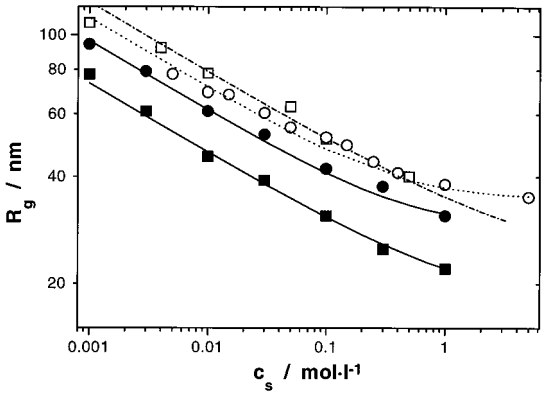

Figure 10. Ionic strength dependence of the radius of gyration for sodium poly(styrenesulfonate)s. Open symbols represent literature values: (□) $M_w = 10^6$ g/mol, Borochov and Eisenberg;[38] $M_w = 7.8 \times 10^5$ g/mol, Peitzsch et al.[10] Present work: (●) $M_w = 570\,000$ g/mol, (■) $M_w = 400\,000$ g/mol.

It is interesting to note that also the co-ions slightly influence the "solvent quality" in terms of w_0. As shown in Figure 9 for the Et-PVP18000Br the solvent quality in the high salt regime increases in the sequence $Na^+ > K^+ > Cs^+ \approx Li^+$ whereas at low c_s no differences in R_g are detected. Thus, the thermodynamic properties of the polyion are somewhat influenced by the co-ions, whereas the thermodynamic *and* the electrostatic behavior is strongly governed by the gegenions.

Comparison to Sodium Poly(styrenesulfonate). In order to demonstrate the general applicability of the theoretical approach we collected literature data on poly(styrenesulfonate) (PSS), a frequently investigated polyion. As already stated in a recent review article,[1] light-scattering investigations on PSS performed by different groups show significant deviations. In Figure 10 we present the supposedly most reliable data as judged by the concentrations at which measurements were performed, i.e., $c_p^m \ll c_s$. Each set of data is perfectly fitted by the theory, however, with a significantly different set of parameters, whereas Peitzsch et al.[10] data are fitted best with $f = 0.32$ and $w_0 = 0.35$ and Borochov and Eisenbergs[38] data yield $f = 0.29$ and $w_0 = 0.05 \pm 0.05$. The difference between the two fits are well outside of the experimental error. In order to clarify the observed discrepancies we decided to perform some additional measurements on two commercially available PSS samples of different molar masses. The results are shown in Figure 10 along with the best fits to eq 4. It is recognized in Table 7 that the parameters f and w_0 of the higher molar mass sample are very close to those obtained from the data reported by Peitzsch et al. data while the f and w_0 values for the smaller molar mass sample are almost indistinguishable from those derived from Borochov and Eisenbergs data. This is quite surprising because at least for the present PSS samples the different sets of f and w_0 values could not be deducted from the sample characteristics in terms of the chemical charge density, i.e., the degree of

Table 7. Fit Parameter *f* and w_0 for Literature and Preset Data on Sodium Poly(styrenesulfonate)

$_w$/gmol^{-1}	*f*	w_0
4.0×10^{-5} [a]	0.3	0.05
5.7×10^{-5} [a]	0.35	0.35
7.8×10^{-5} [b]	0.32	0.35
9.8×10^{-5} [c]	0.29	0.05

[a] Present work. [b] Peitzsch et al.[10] [c] Borchov and Eisenberg.[38]

sulfonation which is above 90% for both samples. Both values for w_0 are above zero, indicating that NaPSS is not salted out in concentrated NaCl solution, in contradiction to literature results where Θ conditions at 4.17 M NaCl are reported.[39] In this respect it should be mentioned that the presently investigated samples (once dissolved) do not precipitate in saturated NaCl solution (i.e., $c_s = 5.0$ M) nor do the solid samples dissolve in saturated NaCl solution.

One possible explanation for the observed differences could be the onset of aggregation at such high salt concentrations which might be induced by subtle differences in the solution preparation or in the sample characteristics such as molar mass or degree of sulfonation, the latter of which always exhibits an uncertainty of 10% (see Experimental Section for the PVP samples). However, a careful analysis of the correlation functions demonstrated the normalized second cumulant for the PSS400 sample to be in the regime $0.0 \leq \mu_2 \leq 0.02$ at all salt concentrations which renders the decay as strictly monoexponential. Sample PSS780 exhibited significantly larger values of $0.02 \leq \mu_2 \leq 0.05$ at $c_s >$ 0.1 M which slightly increased to $0.05 \leq \mu_2 \leq 0.08$ at smaller salt concentrations, i.e., $c_s \leq 0.01$ M. Although it seems tempting to interpret such tiny differences, the following observations certainly obscure any further discussion: For both PSS-samples at $c_s \leq 3 \times 10^{-3}$ M particle clouds were observed to migrate through the light-scattering cuvette (very much like schlieren) and accordingly also to enter the scattering volume leading to an increase in the scattering intensity by up to a factor of 2. These clouds could never be completely removed by extensive filtration and appeared constantly though more or less pronounced. Accordingly, our own data shown in Figure 10 were selected from a large set of measured data or taken under constant visual inspection of the scattering volume. It eventually turned out that both of our PSS samples purchased from Polymer Standards Services, Mainz, do in fact originate from Pressure Chemical Co., Pittsburgh. Therefore, the PSS sample investigated by Peitzsch et al.[10] and our sample PSS780 could come from the same batch. The somewhat lower values of the radii of gyration as compared to the data by Peitzsch et al. seem to be at least consistent with the lower mass of $M_w = 570\,000$ g/mol as compared to $M_w = 780\,000$ g/mol given by the supplier, if degradation of our PSS780 sample had occurred. This would limit the abnormally high w_0-values to be measured on one (artifactual) PSS sample only, whereas Borochov and Eisenbergs and our data on PSS400 yield almost identical and more meaningful w_0-values. At this point we came to the conclusion that sodium poly(styrenesulfonate) might not represent the ideal model polyelectrolyte and refrained from further investigations.

Critical Discussion Concerning the Physical Significance of the Fit Parameter. With the exception of the high molar mass and low ionic strength regime the excluded volume theory presented above almost perfectly describes the experimental data in terms of the "effective" charge density *f* and the intrinsic excluded volume w_0. Such excellent fits, however, do not necessarily prove the fit parameters derived to the physically meaningful. Although the present paper will not give a conclusive answer to this question, we still wish to present some arguments in respect to the applicability of the underlying theoretical concept.

Charge Density *f*. According to Tables 4 and 6 the effective charge density of the investigated samples decreases with increasing hydrophobicity and with decreasing polarization of the gegenion. To the best of our knowledge all analytical theories and simulations so far treat the gegenions as point charges and different polarizabilities are ignored. Likewise, Mannings condensation theory does not predict the charge density along a charged cylinder to depend on the "local dielectric constant" close to the surface but only on the continuous dielectric constant of the medium between the cylinders. At least the latter argument could question the values for *f* to be physically realistic. Although true charge densities will be quantitatively accessible by future electrophoretic mobility measurements, we here wish to present some evidence for and against *f* to be physically realistic.

As has been frequently shown and already discussed in the Experimental Section a slow mode is observed by dynamic light scattering if the polyion concentration exceeds a certain value which is proportional to the added salt concentration. Typically, this ratio $\lambda = c_p^m/c_s$ is in the order of 1 for fully charged polyelectrolytes (i.e., $Q = 100\%$) where c_p^m is defined as the molar concentration of the monomers (charged and uncharged) of the polyion in the solution ("monomoles/*l*").With one exception[40] the question whether c_p^m has to be replaced by the concentration of the chemically charged monomers for polyion charge densities smaller than 1 or by the physically effective ion concentration along the polyion chain is experimentally not precisely addressed in the literature, although dynamic coupling of the counterion and polyion diffusion coefficients is theoretically predicted to be a universal function of the physically effective charge concentration originating from the polyions divided by the ionic strength of the solution.[41,42] In ref 18 the onset of the splitting of the diffusion coefficient was demonstrated to be independent of the chemical charge density which was always significantly larger than the Manning condensation limit. In this former work $\lambda = c_p^m/c_s$ as defined above. This result is taken as a first hint that universal behavior is to be expected if λ is defined in terms of the physically effective charge concentration, i.e., $l = fc_p^m/c_s$. This question is addressed in more detail in Figures 11a−c for measurements on a variety of different samples and solvents, where λ is varied from $\lambda = Q_{EA}c_p^m/c_s$ (Figure 11a, utilizing the "chemical" charge fraction) to $\lambda = f_{MC}$ c_p^m/c_s (Figure 11b, taking the physically effective charge fraction according to Mannings condensation theory, i.e., $f_{CM} = 0.35$) to $\lambda = f_{ex}c_p^m/c_s$ (Figure 11c, adopting the physically effective charge fraction as determined experimentally in this work, see Tables 4−6). In Figure 11b,c, the fast modes show universal behavior within experimental error which makes the derived charge densities, f_{ex}, at least as realistic as Mannings counterion condensating f_{MC}. For the slow modes Figure 11c exhibits even a better superposition of the data. The slow mode measured in MFA is not

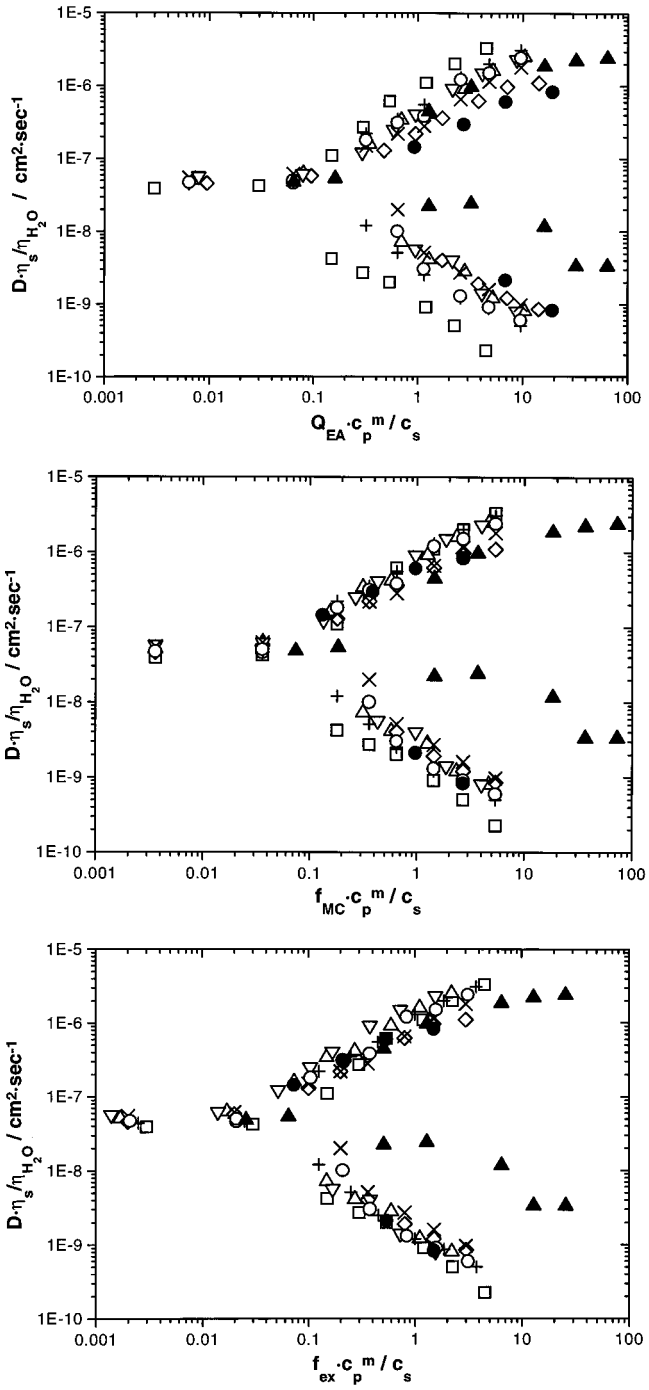

Figure 11. Slow and fast diffusion coefficients normalized to the solvent viscosity of water as a function of different master variables: (a) $Q_{EA}c_p^m/c_s$ with Q_{EA} the chemical charge density determined by elemental analysis, (b) $f_{MC}c_p^m/c_s$ with f_{MC} the physical charge density according to Mannings condensation theory, and (c) $f_{ex}c_p^m/c_s$ with f_{ex} the experimentally determined charge density according to Tables 4−6. The open symbols represent data for sample Al-PVP18000X measured in a 0.01 M aqueous NaBr solution (Al/X⁻): (□) H/Br, (○) Et/Br, (Δ) Bu/Br, (▽) Oc/Br, (◇) Bz/Br, (+) Et/Cl, (×) Et/J; (●) sample Et-PVP18000Br in methanol, c_s = 0.01 M NaBr; (▲) sample Bz-PVP21000Br in methylformamide, $c_s = 10^{-3}$ M NaBr.

expected to show universality because of the different chain length of the sample (see discussion below on Slow Modes).

It should be critically noted that the experimental f values are derived with the assumption that the effective charge density on the polyion does not depend on the added salt concentration. The good theoretical fits shown in Figures 3−5 support this assumption.

***w*₀ Parameter.** The detailed discussion of the w_0-values appears to be similarly delicate. The underlying assumption that w_0 does not depend on the added salt concentration seems to be disproved by the present data as discussed in connection to the increasing solvent quality with increasing added salt for sample Et-PVP10000Br (Figure 8) and for samples Et-PVP18000Br and Bu-PVP18000Br (Figure 6). However, essentially all fits are based on data recorded at $c_s \leq 1$ M added salt corresponding to a salt content of ≤2% (mol of salt/mol of H_2O). Thus, the overall solvent quality might be expected not to vary too much, although preferential adsorption effects may locally increase the solvent quality in the vicinity of the polyion.

Besides this issue, most of the w_0-values lie slightly below or above zero, indicating that aqueous salt solutions are not as bad a solvent for the polyions than is generally anticipated. It is to be noted, however, that the hypothetically uncharged chain does still contain the nondissociated ion pairs (representing large dipoles along the chain) which may in fact drastically increase the solubility in polar solvents. In this respect the present theoretical treatment of the data for the chemically not fully ionized samples is not adequate because two different w_0 values ought to be introduced for the chemically charged and the uncharged groups, respectively. Clearly, such a maneuver appears not to be conceivable for the present set of data.

We still wish to stress the point that the w_0-values as given in the tables thus far seem to be in the correct order, qualitatively.

Slow Modes. The universality demonstrated by Figure 11c deserves a more detailed discussion in respect to the slow mode. The occurrence of both fast and slow modes in polyelectrolyte solutions continues to be an exciting subject for both experimental[1,9−11,13,17−19,43−47] and theoretical[41,42] investigations. Most of the data shown in Figure 11 date from 1993/94 and were never meant to be published, because of the apparent lack of universality as shown in Figures 11a,b. It is the recent reinterpretation of the experimental data in terms of the excluded volume concept, only, which leads to the following most surprising evidence: Not only the fast modes but also the slow modes seem to be a universal function of $\lambda = f_{ex}c_p^m/c_s$ irrespective of the hydrophobicity of the polyion when measured in water and irrespective of the very different physical properties of the solvents used (MeOH, H_2O, and MFA) in agreement with literature.[48] This universality is not only observed in respect to the onset of splitting but also for the absolute values of the hydrodynamic radius associated with the slow diffusion mode if the data are recorded at constant background ionic strength, i.e., $c_s = 10^{-2}$ M for all data except for the measurements in MFA which were taken at $c_s = 10^{-3}$ M. Please note that all diffusion coefficients in Figures 11a−c are normalized to the viscosity of water; i. e., the effect of different solvent viscosities on the diffusion coefficient is eliminated. However, the absolute value of the slow mode does depend on the ionic strength of the solution as was shown earlier.[18] This is also documented by the present data measured in MFA.

Unfortunately, earlier measurements of the Bz-PVP1800Br sample (P3Q3 in ref 18) in a 10^{-3} M aqueous salt solution cannot be compared to the present data taken in MFA, because the slow mode significantly depends on the molar mass or chain length which is 10

Table 8. Ionic Strength Dependence of R_g and R_h (in nm) for Differently Quaternized Samples

H-PVPL_wBr

	R_g					R_h				
Lw/A	1 M	0.3 M	0.1 M	0.03 M	0.01 M	1 M	0.3 M	0.1 M	0.03 M	0.01 M
4000	16.8 ∓ 0.6	18.6 ∓ 1	23.9 ∓ 0.9	27.4 ∓ 0.5		10.3	11.9	13.9	16.9	
6900	23.4 ∓ 0.8	27.7 ∓ 0.8	33.2 ∓ 1	41.1 ∓ 0.5	50.9 ∓ 0.8	13.9	16.2	19.3	22.9	26.2
10000	29.1 ∓ 0.7	33.3 ∓ 0.6	42 ∓ 1	51.4 ∓ 0.8	66.5 ∓ 0.9	18	21.1	24.1	30.6	35.2
18000	42.1 ∓ 0.5	50.7 ∓ 0.5	62.6 ∓ 0.8	82.2 ∓ 1.1	104.5 ∓ 1.4	26.6	32.5	37.6	46.6	55
21000	43.4 ∓ 0.8	51.7 ∓ 0.8	64.4 ∓ 0.9	84.7 ∓ 1	110 ∓ 1.5	25.4	30.8	38	43.3	55.9

Et-PVPL_wBr

	R_g							R_h						
L_w/Å	1 M	0.3 M	0.1 M	0.03 M	0.01 M	0.003 M	0.001 M	1 M	0.3 M	0.1 M	0.03 M	0.01 M	0.003 M	0.001 M
4000	15.2 ∓ 0.6	17.6 ∓ 0.5	22.1 ∓ 0.5	28.8 ∓ 0.5	34.6 ∓ 0.8	41.6 ∓ 0.7	50.7 ∓ 0.8	10	11.4	13.5	15.8	17.4	20.3	(23.5)
10 000	27.5 ∓ 0.5	29.3 ∓ 0.5	36.2 ∓ 0.5	46.6 ∓ 0.6	58.4 ∓ 1	75 ∓ 0.8	95 ∓ 2	18.2	18.9	22.2	26.7	32.5	39	45
18 000	39.6 ∓ 0.5	43.8 ∓ 0.5	54.6 ∓ 0.7	69.9 ∓ 0.7	87.3 ∓ 1	116 ∓ 1.5	145 ∓ 2	26.2	29.7	34.9	41.5	48.8	60.1	74

Bz-PVPL_wBr

	R_g					R_h				
L_w/Å	0.1 M	0.03 M	0.01 M	0.003 M	0.001 M	0.1 M	0.03 M	0.01 M	0.003 M	0.001 M
4000	18.3 ± 0.6	25.6 ± 0.7	30.6 ± 0.4	39 ± 0.7	47.6 ± 1	10.8	14.2	16.4	19.8	
6900	23 ± 0.8	35 ± 0.7	41 ± 0.9	54 ± 1	68 ± 1	14.3	19.3	22.8	27.8	31.6
10 000	27.9 ± 0.8	42.4 ± 0.8	53.5 ± 0.9	69.6 ± 1	91.1 ± 1.5	17.9	24.5	29	36.1	41.3
18 000	43.4 ± 1	65.1 ± 0.7	83.4 ± 1	113 ± 2	140 ± 2	27.5	37	46.6	57.2	66.6
21 000	46.7 ± 0.8	69.9 ± 0.7	91.6 ± 1.5	125 ± 1.5	158 ± 3	28.8	41.2	50	62	74

Table 9. R_g and R_h for Sample Et-PVP10000X for Different Gegenion X^{-1}

Et-PVP10000

	R_g				R_h			
c_s/(mol/L)	NaF	NaCl	NaBr	NaJ	NaF	NaCl	NaBr	NaJ
1		31.6 ∓ 0.8	27.5 ∓ 0.5			19.3	18.2	
0.3	41 ∓ 0.6	34.9 ∓ 0.5	29.3 ∓ 0.5		25.6	21.3	18.9	
0.1	47.2 ∓ 0.5	41.6 ∓ 0.8	36.2 ∓ 0.5	28.3 ∓ 0.8	27.9	24.5	22.2	17.2
0.03	53.7 ∓ 1	50.6 ∓ 0.5	46.6 ∓ 0.5	41.2 ∓ 0.4	32	28.5	26.7	24.8
0.01	66 ∓ 1	61.5 ∓ 0.5	60 ∓ 1	54.9 ∓ 0.7	34.7	33.8	32.5	28.6
0.003	86.5 ∓ 1	78.5 ∓ 0.7	75 ∓ 0.7	73.1 ∓ 0.6	42.8	39.7	39	36
0.001	107 ∓ 1	97 ∓ 1	95 ∓ 1.5	93.5 ∓ 1.5	49	46	45	44

Table 10. Ionic Strength Dependence of R_g and R_h (in nm) for Polyions of Different Hydrophobicity (Sample X-PVP18000Br)

	R_g						R_h					
c_s/(mol/L)	H-PVP	Et-PVP	Bu-PVP	Oc-PVP	Do-PVP	Q-PVP	H-PVP	Et-PVP	Bu-PVP	Oc-PVP	Do-PVP	Q-PVP
1	42.1 ∓ 0.5	39.6 ∓ 0.7	33.6 ∓ 0.6				26.6	23.9	20.8			
0.3	50.7 ∓ 0.5	43.8 ∓ 0.7	36.3 ∓ 0.6				32.5	26.4	23.7			
0.1	62.6 ∓ 0.8	54.8 ∓ 0.6	48.1 ∓ 0.4	42.4 ∓ 0.6	18.4 ∓ 0.6	43.4 ∓ 0.8	37.6	31.3	28.6	26.4	14.6	27.5
0.03	82.2 ∓ 1.1	69.9 ∓ 0.7	62.5 ∓ 0.7	59 ∓ 0.7	26.7 ∓ 0.6	65.1 ∓ 0.5	46.6	39	34.6	34.9	17.7	37
0.01	104.5 ∓ 1.4	87.3 ∓ 1	79.1 ∓ 0.7	73.3 ∓ 0.6	36.5 ∓ 1	83.4 ∓ 1	55	45.6	42.1	39	21.2	46.6
0.003	140 ∓ 2.5	116 ∓ 1.5	105 ∓ 1.5	94.4 ∓ 1.5	48.1 ∓ 1	113 ∓ 2		59.5	49.9	46.6	24	57.2
0.001	180 ∓ 3	145 ∓ 1.5	138 ∓ 2	124 ∓ 2	61 ∓ 1	141 ∓ 2		73	58	55	28.8	66

êtimes larger for the presently investigated sample. Still, the fast mode, i.e., coupling phenomena, seems not to be influenced by the choice of the solvent nor by different chain length.

A clear tendency is observed toward the amplitude of the slow mode as compared to that of the fast mode, which decreases in the sequence MFA > H_2O ≫ MeOH and seems to be qualitatively related to the dielectric constant of the solvent. The present data are in clear contradiction to the speculation that the slow mode originates from a peculiar "hydrophobic" effect connected to the structure of water. Rather, the "universal" size of the not yet identified objects seem to support the hypothesis that electrostatically interacting clusters are formed for some reason. A plausible theoretical argument for this effect has been recently attempted.[42]

Acknowledgment. We thank Dr. R. Richert and X. Yan, MPI für Polymerforschung, Mainz, for determining the dielectric constants of the solvents. Practical and administrative support of Dr. K. Fischer is greatly appreciated. Financial support of the "Fonds der Chemischen Industrie", of the Deutsche Forschungsgemeinschaft (Schwerpunkt Polyelektrolyte), of the Center of Materials Science at the University of Mainz and of the NSF Grant No. DMR-962548−5 is gratefully acknowledged.

Appendix A

The alternative procedure for analyzing the experimental data is to utilize the theory of excluded volume on electrostatically stiffened polyelectrolytes as given by eqs 9−16. As already discussed, these equations are valid only if the electrostatic persistence length given by eq 10 is less than the intrinsic persistence length l_p. In fact, for the experimental conditions investigated in this paper, the constraint of $l_e < l_p$ is satisfied only for $c_s \geq 0.05$ M. The majority of our experimental data are recorded in the range of salt concentrations where eqs 9−16 are not valid. Nevertheless, there have been

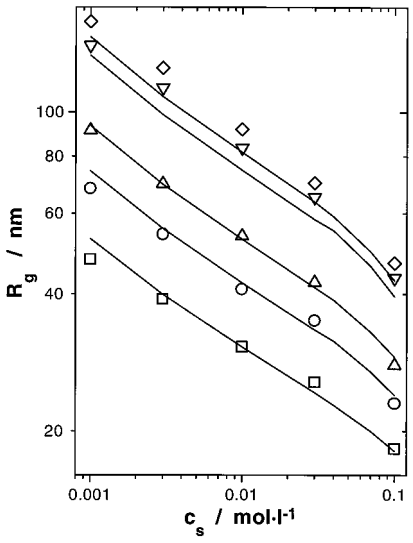

Figure 12. Fit examples (solid lines) for sample Bz-PVPL_wBr with the combined OSF/excluded volume approach, i.e., eqs 9−16, with $l_p = 20$ Å and $V_0 = -10\,000$.

attempts in the literature to simply use eqs 9−16 to fit the data even for situations where the calculated l_e is larger than l_p. In view of this practice, we present a fit of our experimental data by eqs 9−16. Although the fit appears to be good, as shown in Figure 12 for the Bz-PVP samples, the values of the parameters (f,β_0,l_p) needed for the fit are unrealistic. For example, the intrinsic persistence length of the hypothetically uncharged polymer needs to be 25 and 34 Å, respectively, for Bz-PVP and H-PVP. Such unreasonably high values for the intrinsic persistence length have also been reported by Reed et al.[9,10] using the same fitting procedure, i.e., 32 and 37 Å, respectively, for the intrinsic persistence length of poly(styrenesulfonate) and acrylamidesodium acrylate copolymers.

Appendix B

The data given in this work may well be relevant for future theoretical studies, particularly on the dynamic behavior of polyelectrolytes. We hope that our data will stimulate a quantitative comparison between available theories and data. Therefore we simply present the data in the form of compact tables (Tables 8−10) without further comment.

References and Notes

(1) Förster, S.; Schmidt, M. *Adv. Polym. Sci.* **1995**, *120*, 53.
(2) Nagasawa, M.; Takahashi, A. In *Light Scattering from Polymer Solutions*; Huglin, M. B., Ed.; Academic Press: New York, 1972.
(3) Takahashi, A.; Nagasawa, M. *J. Am. Chem. Soc.* **1964**, *86*, 543.
(4) Noda, I.; Tsuge, T.; Nagasawa, M. *J. Phys. Chem.* **1970**, *74*, 710.
(5) Odijk, T. *J. Polym. Sci. Polym. Phys. Ed.* **1977**, *15*, 477.
(6) Skolnick, J.; Fixman, M. *Macromolecules* **1977**, *10*, 944.
(7) Le Bret, M. *J. Chem. Phys.* **1982**, *76*, 6248.
(8) Odijk, T.; Houwaart, A. *J. Polym. Sci. Polym. Phys. Ed.* **1978**, *16*, 627.
(9) Reed, W. F.; Ghosh, S.; Medjahdi, G.; Francois, J. *Macromolecules* **1991**, *24*, 6189.
(10) Peitzsch, R. M.; Burt, M. J.; Reed, W. F. *Macromolecules* **1992**, *25*, 806.
(11) Li, X.; Reed, W. F. *J. Chem. Phys.* **1991**, *94*, 4568.
(12) Ghosh, S.; Kobal, I.; Zanette, D.; Reed, W. F. *Macromolecules* 1993, *26*, 4685.
(13) Ghosh, S.; Li, X.; Reed, C. E.; Reed, W. F. *Biopolymers* **1991**, *30*, 1101.
(14) Fouissac, E.; Milas, M.; Rinaudo, M.; Borsali, R. *Macromolecules* 1992, *25*, 5613.
(15) Barrat, J. L.; Joanny, J. F. *Europhys. Lett.* **1993**, *3*, 343.
(16) Stevens M. J.; Kremer, K. *Phys. Rev. Lett.* **1993**, *71*, 2228.
(17) Schmidt, M. *Macromol. Chem. Rapid Commun.* **1989**, *10*, 89.
(18) Förster, S.; Schmidt, M.; Antonietti, M. *Polymer* **1990**, *31*, 781.
(19) Förster, S.; Schmidt, M. Antonietti, M. *J. Phys. Chem.* **1992**, *96*, 4008.
(20) Fixman, M.; Skolnick, J. *Macromolecules* **1978**, *11*, 863.
(21) Barrat, J. L.; Joanny, J. F. *Adv. Chem. Phys.* **1996**, *XCIV*, 1.
(22) Li, H.; Witten, T. A. *Macromolecules* **1995**, *28*, 5921.
(23) Ha, B. Y.; Thirumalai, D. *Macromolecules* **1995**, *28*, 577.
(24) Flory, P. J. *J. Chem. Phys.* **1953**, *21*, 162.
(25) Muthukumar, M. *J. Chem. Phys.* **1987**, *86*, 7230.
(26) Muthukumar, M. *J. Chem. Phys.* **1996**, *105*, 5183.
(27) Kuhn, W.; Künzle, O.; Katchalsky, A. *Helv. Chim. Acta* **1948**, *31*, 1994.
(28) De Gennes, P. G.; Pincus, P.; Velasco, R. M.; Brochard, F. *J. Phys. France* **1976**, *37*, 1461.
(29) Yamakawa, H. *Modern Theory of Polymer Solutions*; Harper and Row: New York, 1971.
(30) Des Cloizeaux, J.; Jannink, G. *Polymers in Solution, Their Modelling and Structure*; Clarendon Press: Oxford, 1990.
(31) Muthukumar, M.; Nickel, B. G. *J. Chem. Phys.* **1987**, *86*, 460.
(32) Gupta, S. K.; Forsman, W. L. *Macromolecules* **1972**, *5*, 779.
(33) Becker, A.; Köhler, W.; Müller, B. *Ber. Bunsen−Ges. Phys. Chem.* **1995**, *99*, 600.
(34) Muller, G.; Ripoll, G.; Selegny, E. *Eur. Polym. J.* **1971**, *7*, 1372.
(35) Beer, M.; Schmidt, M. *Macromol. Chem. Rapid Commun.*, submitted for publication.
(36) Beer, M. Ph.D. Thesis, University Bayreuth, 1996.
(37) Eisenberg, H.; Mohan, G. R. *J. Phys. Chem.* **1959**, *63*, 671.
(38) Borochov, N.; Eisenberg, H. *Macromolecules* **1994**, *27*, 1440.
(39) Takahashi, A.; Kato, T.; Nagasawa, M. *J. Chem. Phys.* **1967**, *71*, 2001.
(40) Topp, A.; Belkoura, L.; Woermann, D. *Ber. Bunsen−Ges. Phys. Chem.* **1995**, *99*, 730.
(41) Schmitz, K. S. *An Introduction to Dynamic Light Scattering by Macromolecules*; Academic Press: New York, 1990.
(42) Muthukumar, M. *J. Chem. Phys.* **1997**, in press.
(43) Sedlak, M.; Amis, E. J. *J. Chem. Phys.* **1992**, *96*, 817 and 826.
(44) Gosh, S.; Peitzsch, R. M.; Reed W. F. *Biopolymers* **1992**, *32*, 1105.
(45) Sedlak, M. *Macromolecules* **1993**, *26*, 1158.
(46) Reed, W. F. *Macromolecules* **1994**, *27*, 873.
(47) Sedlak, M. *J. Chem. Phys.* **1996**, *105*, 10123.
(48) Sedlak, M. *J. Chem Phys.* **1994**, *101*, 10140.

MA9709821